Using Modeling to Understand the Hygromechanical and Hysteretic Behavior of the S2 Cell Wall Layer of Wood

Dominique Derome, Karol Kulasinski, Chi Zhang, Mingyang Chen and Jan Carmeliet

Abstract To understand moisture sorption and swelling of wood requires revealing the behavior at the S2 cell wall layer, one of the layers of the secondary cell wall, at the atomistic scale. Difficulties in experimentally determining the organization and properties of S2 layer at such a small scale are a stumbling block for understanding of swelling and sorption in their full complexity. Recent works using atomistic modeling (Molecular Dynamics (MD) and Grand Canonical Monte Carlo) provide complementary insights. The linear dependence between moisture content, swelling, and porosity change is found to be correlated with the number and location of water–polymer hydrogen bonds within the system. Such information is upscaled for general use within a poromechanical framework. This chapter summarizes recent new physical insights in the sorption and swelling behavior of the S2 cell wall layer, stemming from validated MD work. The presented methodology is also used to unravel other moisture-related mechanisms of wood, such as hysteretic behavior.

D. Derome (✉) · C. Zhang · M. Chen
Laboratory of Multiscale Studies of Building Physics, Empa, Dübendorf, Switzerland
e-mail: Dominique.Derome@empa.ch

K. Kulasinski
Department of Geochemistry, Lawrence Berkeley
National Laboratory, Berkeley, CA, USA

C. Zhang · M. Chen · J. Carmeliet
Chair of Building Physics, Department of Mechanical and Process Engineering,
ETH Zürich, Zürich, Switzerland

Introduction

Wood, an orthotropic cellular biomaterial, has the capacity of adsorbing water molecules from the surrounding environment into its hierarchical material structure. As water molecules attach themselves to the hydrophilic matrix in the cell walls, the induced fluid–solid interaction forces result in a swelling of the cell walls. Moisture-induced internal stresses due to restrained swelling highly influence the hygromechanical behavior of wood as observed at the macroscale. Adsorption of moisture in wood, in the hygroscopic range, i.e., until around 30% moisture content mass per mass, results in swelling up to 10% volumetrically and reduces the stiffness depending on the grain direction, with, e.g., a decrease of 20% in the longitudinal direction and by half in the radial and tangential directions between 5 and 25% MC for spruce (Neuhaus 1981, Forest Products Laboratory 2010).

Wood structural higher hierarchical levels can be considered as lumber, growth ring, cell, and layered cell wall material. The variation of the cellular structure across the growth ring has been found responsible, at least in part, for the anisotropy of swelling and stiffness (Boutelje 1962; Watanabe et al. 2000). From cellular and subcellular investigations, it has become clear that the microscopic origin of swelling lies at the scales of the cell wall composite material.

The cell wall of sclerenchyma cells is composed of four layers built as exoskeleton of the cell. The primary (P) layer is the first layer which is produced as the cell is growing. At mature stage, the cell builds its secondary (S) layer in three phases. The thin internal and external cell wall layers (i.e., S3 and S1) act as restraining corsets due to the winding of the cellulose microfibrils around the cell. In the central and, by far, thickest cell wall layer, namely S2, the cellulose microfibrils are almost parallel to the longitudinal axis of the cells, although the presence of an angle (called microfibril angle, MFA) results in a helicoidal organization of the fibrils. The hypothesis, that microfibrils were parallel to each other, is presently challenged as speculations of more complex configurations tend to be confirmed lately with tomographic transmission electron microscopy (Xu et al. 2007) or as developed by Salmén and Burgert (2009).

The cell wall composite material is made of the stiff cellulose microfibrils, mentioned above, embedded in a soft polymeric matrix, as shown in Fig. 1a. The microfibrils are made of crystalline cellulose (hydrophobic or hydrophilic depending on the surfaces of the crystal, where crystal dimensions are roughly $3 \times 3 \times 25$ nm) bound by hydrophilic amorphous hemicellulose, thus making long thin filaments. Amorphized cellulose may occur at this crystal/hemicellulose interface. These microfibrils can form bundles, named aggregates. Microfibrils and aggregates lie within the hydrophilic amorphous matrix, composed of different hemicelluloses and lignins. Hemicelluloses of interest here are galactoglucomannan and arabinoglucoronoxylan (Salmén 2004). Measurements indicate that the components closest to the microfibrils are somewhat oriented along these, while an orientation is not found for components lying in the center of the inter-microfibril matrix (Salmén and Burgert 2009). Still, the object of debate (Eichhorn 2011; Cosgrove 2014), the chemical components of the
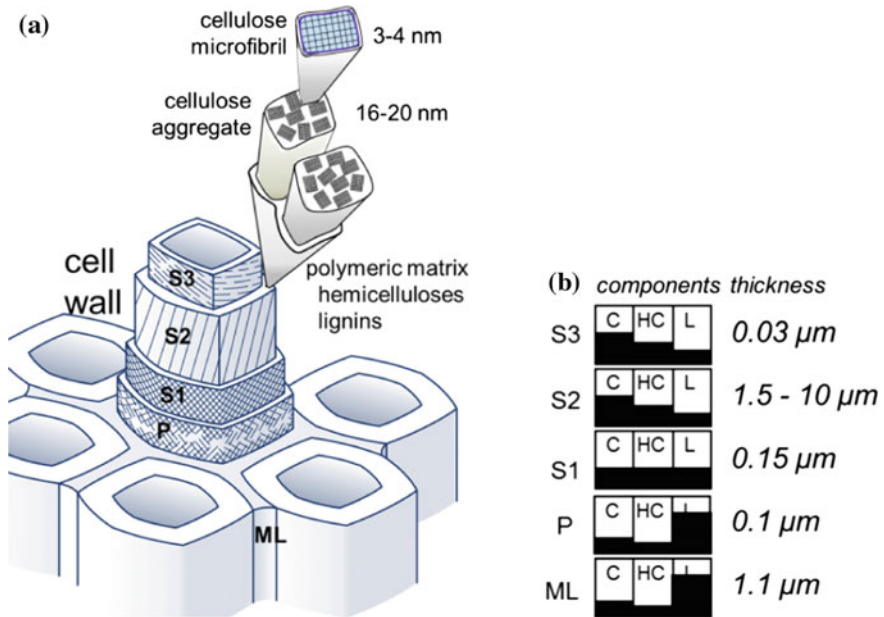
Fig. 1 **a** Schematic representation of the structure of the wood cell walls, with P primary layer, S secondary layer, ML middle lamella, **b** schematic representation of the proportion of cellulose (C), hemicelluloses (HC) and lignins (L) in the different cell wall layers and their thickness (Derome et al. 2012, with permission)

S2 layer and their relative configuration are progressively elucidated. Nevertheless, the distance between cellulose microfibrils is estimated to be in the order of 4–10 nm in dry cell walls and filled with the amorphous matrix (Dinwoodie 2000; Fahlén and Salmén 2005; Höfter et al. 2007). Proportion of the cellulose (C), hemicelluloses (HC), and lignins (L) are given schematically for each wall layer in Fig. 1b, showing that, overall, the cell wall material is composed in almost equal share of stiff cellulose microfibrils and soft polymeric matrix.

Experimental evidence of swelling has been long attained at wood scale. In particular, at the cellular tissue scale, a series of phase contrast synchrotron X-ray tomography (at the Tomcat beamline, Swiss Light Source, Paul Scherrer Institute) has been performed to identify the role of growth ring and cellular geometry in terms of effects on swelling, swelling anisotropy as function of density and hysteresis in swelling due to sorption hysteresis (Derome et al. 2011; Patera et al. 2013 and illustrated in Fig. 2a, b). Careful geometry analysis of the hierarchical structure of wood tissues is performed during moisture-induced deformations (swelling/shrinkage) at cellular and sub-cellular scales. Swelling in adsorption and shrinkage in desorption displays hysteresis, with higher deformation in desorption than in adsorption at the same relative humidity. Moisture content curves are also hysteretic with higher moisture content in desorption than in adsorption for the same relative humidity. However,

softwood swelling is found to be non-hysteretic when considered in terms of moisture content highlighting the capacity of wood to deform similarly for the same moisture content and independently of moisture history. Further, these experimental results show that anisotropy in swelling in the cross-sectional directions is function of density, where the swelling of earlywood is restrained in the radial directions, whereas the latewood, given its bulky structure, deforms quite isotropically. Further, work using phase contrast synchrotron X-ray nanotomography captured the swelling of the isolated cell wall materials, sculpted as pillars with focused ion beam, using micropillars of the S2 layer (Fig. 2c and Rafsanjani et al. 2014) and of the middle lamella (ML) layer (Fig. 2d and Patera 2014) and subjecting them to different relative humidity. Observations reveal an anisotropic swelling in the S2 layer sample and an isotropic swelling in the ML sample, i.e. made of cell binding material which does not contain microfibrils. This indicates that swelling is driven from a sub-cellular scale. To summarize, Fig. 3 shows how wood structure constrains the swelling of its base material, with swelling coefficients for the S2 micropillars demonstrating a much higher volumetric swelling than those of the cellular tissues, either from earlywood or latewood. At cellular scale, the corset action of the S1 and S3 layers must enter in play. At timber scale, in presence of growth rings, this swelling is even further constrained.

Water molecules can easily form hydrogen bonds with the hydroxyl groups of the amorphous components. For example, amorphous cellulose is a strongly hydrophilic biopolymer (e.g., Beever and Valentine 1958) due to its open porous structure and the presence of exposed hydroxyl (O_2 and O_3) and hydroxymethyl (O_6) groups. Thus, as the adsorption process involves mainly atomistic interactions, molecular dynamics (MD) simulations are an appropriate tool for its investigation. Typical scales of the process range from angstroms to micrometers. Contrary to mesoscale methods, such as coarse grain MD, atomistic MD can capture hydrogen bonds formation and dipoles interaction and, unlike better resolution methods (e.g., DFT, generally limited to sizes of hundreds of atoms and time-scales of picoseconds), MD enables simulation of larger structures (up to millions of atoms) and at larger time scales (up to µs). For the problem of moisture-related behavior, atomistic MD offers several advantages. First, it allows full consideration of explicit water molecules. As such, MD can deliver information on hydrogen bonds (Kulasinski et al. 2015a; Nishiyama et al. 2002) and on dipoles of the water molecules (e.g., Teleman et al. 1987; Kulasinski et al. 2015c) and it can track the motion of molecules to document diffusion (Kulasinski et al. 2015d). Second, if needed, MD allows control of atoms as external forces can be applied to a group of atoms, hence enabling experimentally challenging operations, such as polymer chain pulling or free energy determination. Finally, as each component is homogeneous, the properties of each component can be determined by applying periodic boundary conditions on the representative volume element (RVE). This means that atoms in the system interact across the boundary, and they can exit at one end of the system and reenter from the other end. Furthermore, the application of periodic boundary conditions allows determining the long-range electrostatic forces by Ewald summation instead of truncation, which gives a better evaluation of the long-range electrostatic interactions (Oostenbrink et al. 2004; Lins and Hünenberger
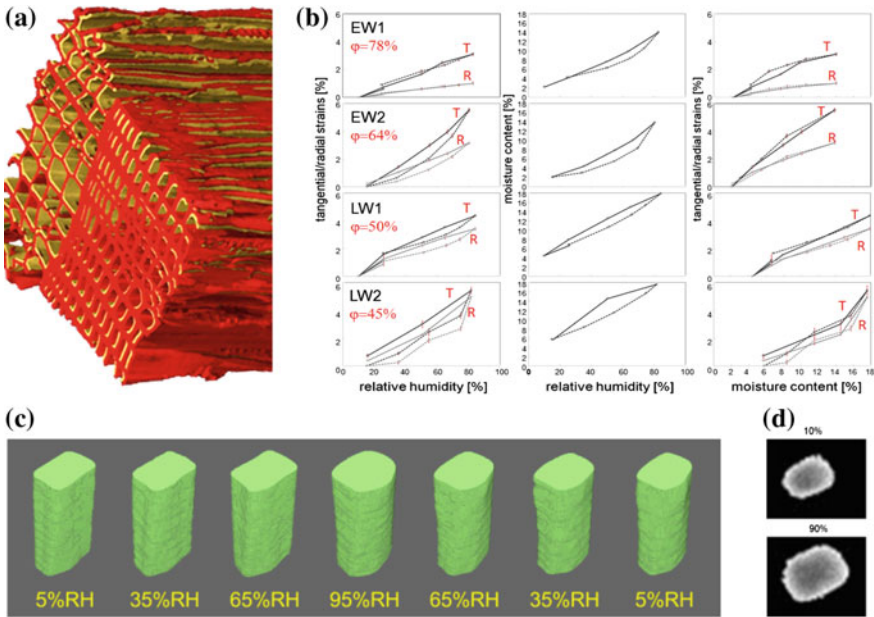
Fig. 2 Imaging using X-ray CT during swelling experiment of **a** cellular structure at growth ring border at 25% (red) and 50% RH (ochre), **b** swelling strains and moisture content versus relative humidity, and swelling strains versus moisture content for 4 homogeneous wood tissues of high to low porosity (φ) (EW earlywood, LW latewood, T tangential, R radial, dashed line in adsorption and solid line in desorption) (from Patera et al. 2013, with permission) **c** S2 micropillar during adsorption and desorption, **d** ML micropillar at 10 and 90% RH (from Patera 2014)

2005). For all these reasons, MD has been used toward studying the S2 cell wall material behavior.

The goal of this chapter is to convey the physical processes at play during water sorption in wood cell wall using the particular lens of recent MD investigations. The specific objectives are as follows:

1. To provide an overview of the method, capacities, and limits of molecular dynamics
2. To display the possible types of investigations and results achievable with this modeling approach when looking at the impact of water on the behavior of the S2 cell wall layer
3. To expose the underlying role of hydrogen bonding, as a unifying agent.
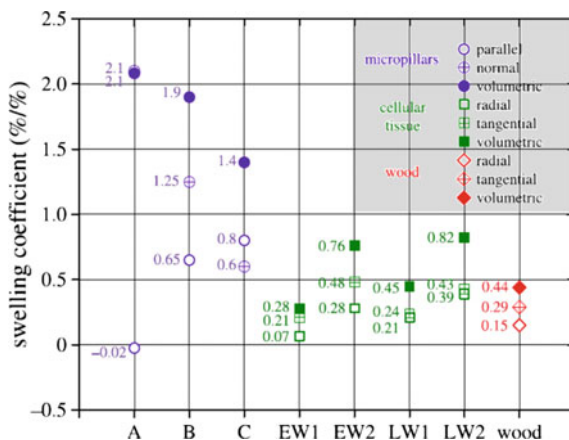
Fig. 3 Comparison of swelling coefficients at three scales: samples A, B, C are S2 micropillars (μm), the next four samples are pure early- or latewood samples (500 × 500 μm) (Patera et al. 2013) and for wood at plank scale cm (Rafsanjani 2013b), all of Norway spruce (from Rafsanjani et al. 2014, with permission)

Methods

Molecular Dynamics

Molecular dynamics simulations are carried out, for the most part, using Gromacs software (Hess et al. 2008) with leap-frog algorithm for integration of Newton's equations of motion and the Gromos 53a6 united-atom force field (Oostenbrink et al. 2004; Lins and Hünenberger 2005). In section "Hysteresis", molecular dynamics simulations are carried out using LAMMPS (Large-Scale Atomic/Molecular Massively Parallel Simulator) (Plimpton 1995) with velocity-Verlet algorithm for integration of Newton's equations of motion and the PCFF (Polymer Consistent Force Field) force field (Sun et al. 1994).

The size of the studied systems (RVE) is in the order of nanometers, counting 10^5 atoms at maximum and the sampling time could reach 20 ns. All MD measurements are carried out at a constant temperature, 300 K, and at constant pressure (using the isobaric–isothermal ensemble NPT, i.e., constant number of atoms, pressure, and temperature, while allowing variation in volume).

The initial configuration of the each polymer is constructed based on the position of atoms in the chains as known from experiments or other MD works, e.g., for xylan (Wagenführ and Scholz 2012; Jin et al. 2015) and for lignin (with predefined sequence used in Charlier and Mazeau 2012; Petridis and Smith 2009; Petridis et al. 2011a, b; Sangha et al. 2012; or dynamic bond-forming procedure used by Jin et al. 2015). This initial structure must then find an equilibrium configuration. The procedure of amorphization of polymeric chains has two stages (Kulasinski et al. 2014a).

First, the polymer is raised to a temperature above its melting point and equilibrated there in stress-free conditions until the chains lose their ordered structure, typically after 1 ns. Then, the amorphized chains are quenched to room temperature and equilibrated in stress-free conditions. For example, for single component, the number of polymer atoms for such simulation is around 3000–5000, resulting in a domain of $3 \times 3 \times 3$ nm^3 and the largest system built to represent the S2 materials, with four cellulose crystal separated by galactoglucomannan and surrounded by lignin, counts close to 38 000 atoms and has a volume of 516 nm^3. Periodic boundary conditions (PBC) are employed in order to mimic bulk material properties, despite the small size of the RVE. For those polymers with their size exceeding the MD box dimensions, the PBC is achieved by covalently bonding the molecules to themselves across the periodic boundary. For the S2 material, the RVE is configured as a unit which, when repeated via the periodic boundaries conditions, yields an acceptable S2 overall configuration.

In order to study the different responses of the polymers to water, e.g., the responses being here mechanical, topological, hygric or thermal, water molecules are introduced to the system (Smith and van Gunsteren 1994). The water model used is the simple point charge water model (SPC) (from Berendsen et al. 1984). The SPC water model has three interaction points corresponding to the three atoms of the water molecule, with point charge on each site. Starting from a dry system, water molecules are inserted one by one at random into the void space between the polymer chains, see Fig. 4. A successful insertion of a water molecule is followed by a relaxation run at stress-free conditions. Relaxation time and temperature usually need to be adapted to each system and moisture content. Once the desired number of water molecules has been inserted and the system allowed to relax, the system is interrogated during production runs (Kulasinski et al. 2014b, 2015a, b, c, d). A hydrogen bond can be recognized when the acceptor and the donor of a couple are within 0.35 nm from each other and the angle between the prolongation of the OH branch with the hydrogen bond is less than 30°, as shown in Fig. 5.

The production runs are used to study the moisture-related behavior of the different polymers and the results are compared with experimental data for validation, as explained below. In particular, the following properties can be determined and are described in more detailed below. Water adsorption isotherms, as shown in Figs. 6 and 7, are obtained using One-Step Perturbation method (Zwanzig 1954) for the determination of chemical potential. Swelling of the system at each water insertion leads to the determination of the dependence of swelling coefficient (Fig. 8) and porosity (Fig. 9) on moisture content. The mean square displacement of the water molecules is used to determine water diffusion coefficient versus moisture content (Fig. 10). Under mechanical loading, i.e., an anisotropic barostat is applied and the pressure is specified, the system finds its equilibrium and a corresponding strain can be measured. The bulk and shear moduli dependence on moisture content can be determined, as shown in Fig. 11.

An analysis of the nanoscopic behavior of polymer–water systems is possible given the unique level of information provided by MD simulations. For example, the shift in the diffusion coefficient dependence is seen to concur with the percolation
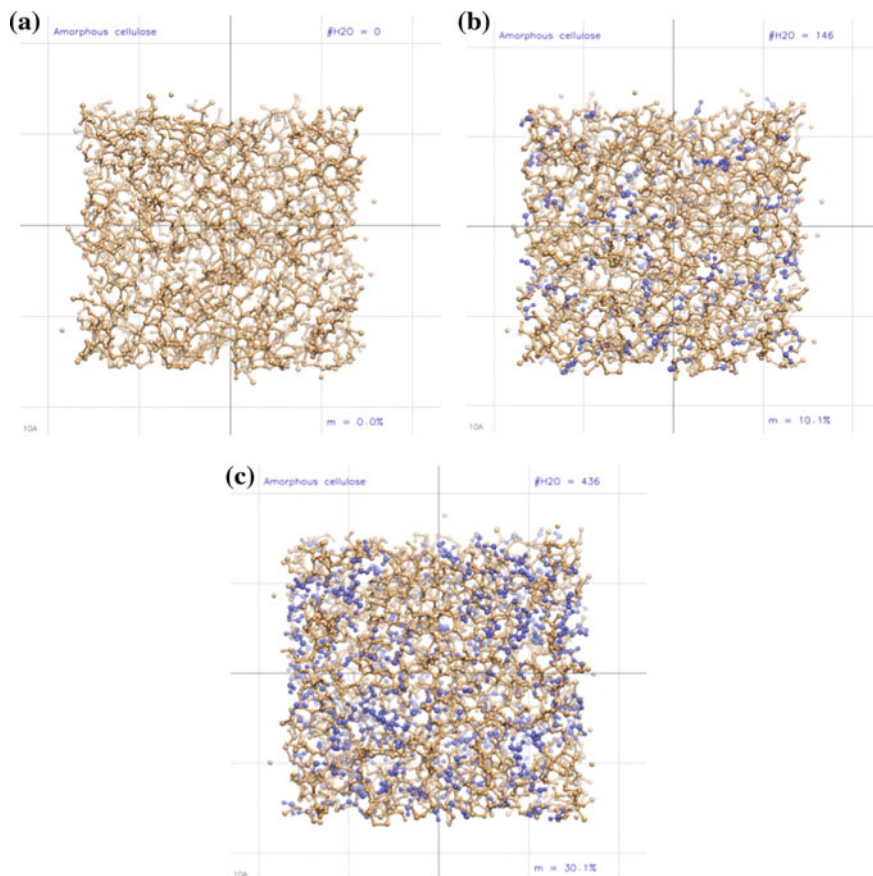
Fig. 4 MD results of amorphous cellulose at different moisture contents, **a** 0%, **b** 10.1, **c** 30.1%

of water molecules through the polymer (Kulasinski et al. 2014b). Another series of analysis can be based on the average lifetime, location and number of hydrogen bonds in the polymeric systems. Comparing the number of hydrogen bonds, as described in Fig. 5, between polymers versus the number of such bonds between polymer and water, can reveal insightful information as shown in Fig. 12.

As mentioned above, the methods described are used to determine the moisture adsorption isotherm, the moisture dependency of swelling, mechanical properties, and diffusion coefficient for all components and systems, in order to have a full characterization of the S2 layer, in addition to a better insight of S2 behavior in contact with moisture. The involved polymers are crystalline cellulose, amorphous cellulose, galactoglucomannan, arabinoglucuronoxylan, condensed lignin, and uncondensed lignin. Cellulose is a polysaccharide consisting of a linear chain of $\beta(1 \rightarrow 4)$ linked D-glucose units. It can form crystalline, paracrystalline, and amorphous states. There are two major species of hemicellulose in softwood, namely galactoglucoman-
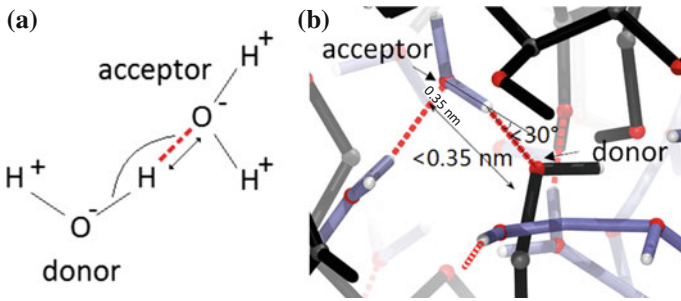
Fig. 5 Criteria of the existence of hydrogen bonds in terms of angle and distance, **a** schematic representation, **b** color visualization in a MD system with hydrogen bonds, shown in red, present between polymers (covalent bonds and carbon shown in black), between polymer and water (with blue bonds between oxygen in red and hydrogen in white) and between water molecules (from Kulasinski 2015 with permission)
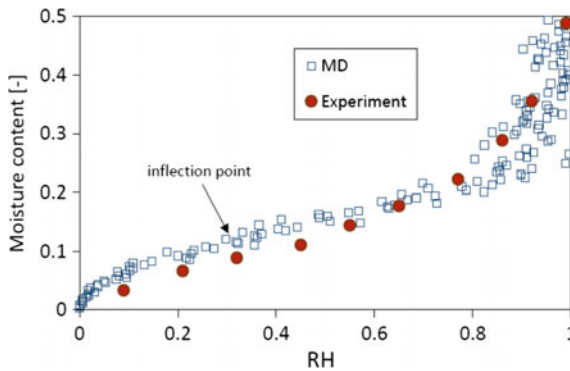

Fig. 6 Validation example of comparison of simulation and experiments results, taken from Beever and Valentine (1958), of the isotherm of amorphous cellulose of moisture content versus relative humidity (RH) (from Kulasinski et al. 2014b with permission). Given the periodic boundary conditions used in MD, the modeled system is considered bulk amorphous cellulose, thus comparable with experiments on bulk amorphous cellulose

nan, which consists of a backbone of randomly distributed $(1 \rightarrow 4)$-linked mannose and glucose units with $(1 \rightarrow 6)$-linked galactose units attached to mannose units, and arabinoglucuronoxylan which consists of a backbone of $\beta(1 \rightarrow 4)$ linked D-xylopyranose with MeGlcA and α-L-Araf residues attached at positions 2 and 3. Softwood lignin majorly consists of coniferyl units. Condensed lignin is a complex randomly branched polymer with several linkage types, e.g., β-O-4, α-O4, β-4, 5-5, and 5-O-4. Uncondensed lignin is more a linear polymer, with majorly β-O-4 linkages.

In addition to the individual components, we introduce three composite systems: a matrix mix of xylan and uncondensed lignin, microfibrils made of galactoglucomannan wrapping crystalline cellulose and S2 understood here to be microfibril

Table 1 Types of studied systems, full names, acronyms and symbols

Type	Class	Full name	Acronym	Symbol
Single component	Cellulose	Crystalline cellulose	CC	—[a]
Single component	Cellulose	Amorphous cellulose	AC	◇
Single component	Hemicellulose	Galactoglucomannan	GGM	○
Single component	Hemicellulose	Arabinoglucuronoxylan	Xyl	●
Single component	Lignin	Condensed lignin	cLGN	□
Single component	Lignin	Uncondensed lignin	uLGN	■
Composite	Matrix	Xyl+uLGN	Matrix	▲
Composite	Microfibrils	CC+GGM (red) as per inset (a) below	μF	☆
Composite	S2	CC+GGM (red)+LGN (black) as per inset (b) below	S2	✶

[a]no symbol as no result of single CC is presented in this chapter

aggregates, where four microfibrils are wrapped by lignin. The list of systems is found in Table 1.

(a)   (b)   10 Å
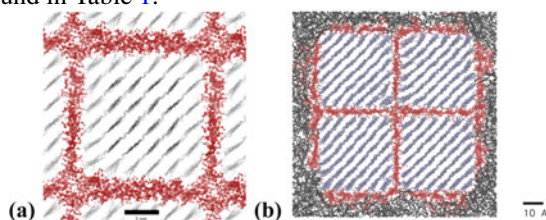
Grand Canonical Monte Carlo

A limitation of applying MD in sorption problems is that the random insertion of water molecules does not recognize the difference of potential fields within different pores. This makes it impossible to distinguish between adsorption and desorption as potential landscapes of the polymer system. To study sorption hysteresis, an alternative way is to include the Grand Canonical Monte Carlo method (GCMC). Instead of imposing a certain number of water molecules and then determining the chemical potential, GCMC operates in an opposite way, that is, the chemical potential is imposed as the boundary condition while the number of the adsorbed water molecules is determined based on statistics of the simulation results. Specifically, after imposing the chemical potential, the GCMC employs the Metropolis algorithm to perform a certain number of trial insertions and removals, which can be accepted or rejected. The acceptation/rejection probability is determined by the chemical potential and the potential landscape within the polymer system. In this way, the difference of potential

landscapes between adsorption and desorption caused by different configurations is taken into consideration so that one can mimic the physical process of adsorption and desorption, respectively, thus with the possibility to describe the hysteretic behavior.

Validation

In the work presented below, the different systems are evaluated in terms of moisture-related behavior by studying the systems at different moisture content. As for any modeling investigation, validation of the work is required. This is done here by comparing the simulation results with experimental values. It was found that MD simulations provide results that are in agreement with experiments, even if the size of a MD model is rather limited, for adsorption isotherms (an example is given in Fig. 6 for amorphous cellulose), mechanical moduli, swelling coefficient, heat of sorption, and diffusion coefficients from experiments carried out using wood or components. This said we note that experimental data at comparable scales or for comparable chemical compositions, as some polymers may undergo modifications during wood extraction, are not abundant.

Results

Sorption

Isotherms provide the total moisture content ($m = (m_{wet} - m_{dry})/m_{dry}$) adsorbed at different relative humidity (RH, the conventional surrogate for chemical potential μ, and $k_B T \ln(RH) = \mu - \mu_{sat}$ with k_B Boltzmann constant, T temperature, μ_{sat} chemical potential of saturated vapor), determined as described above from the chemical potential resulting from the addition of water molecules in the polymeric systems.
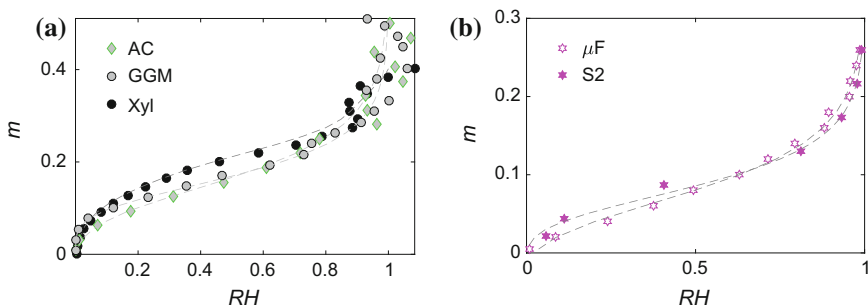

Fig. 7 Adsorption curves for **a** amorphous cellulose and two hemicelluloses, **b** microfibrils and S2 composite systems, in function of relative humidity (RH) (graph **b** from Kulasinski 2015), where m is moisture content

For the single components, we verify that water distribution within the polymer is quite uniform. The sorption isotherms agree with experimental results in terms of the shape of the curve and of the moisture content range attained (Fig. 7a). For the composite systems, we find that more water is adsorbed at the interface between two polymers showing higher water density profiles. Nevertheless, due to the presence of crystalline cellulose which does not absorb any water molecule, the total moisture contents are significantly lower in the microfibril systems than in the single systems (Fig. 7b).

Swelling

The introduction of water molecules results in a displacement of the polymeric systems, as visible in Fig. 4 with the reference geometry given by a red rectangle, leading to an overall material swelling. For the single components and the matrix system, made of amorphous components, swelling is found to be isotropic. Figure 8 shows that volumetric swelling strains (determined by $(V - V_0)/V_0$, where V, V_0 represent the current and dry volumes of the system, respectively) vary linearly with moisture content larger than 17%, the slope of this relationship yielding the swelling coefficient. Swelling coefficients are ranging from 1.07 for S2 to 2.0 for GGM. The different swelling coefficients stem from the combined effects of initial density and porosity, number of hydroxyl sites, and bulk modulus, resulting from the different monomers content and arrangement of each system. We note that the slope at low moisture content is always smaller and nonlinear, this aspect is further discussed in the section "Porosity". The volumetric swelling of S2 layer is found to be smaller than those of hemicellulose and lignin alone. The crystalline cellulose acts as a stiff skeleton preventing the system from deformation. This effect is particularly pro-
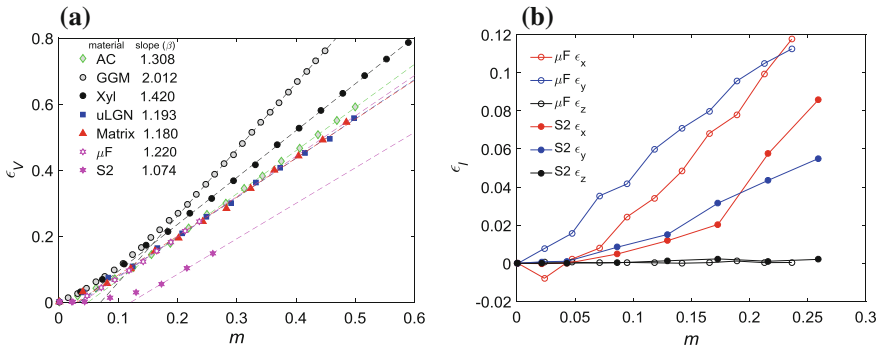

Fig. 8 **a** Volumetric swelling strain (ε_V) of four polymers and one amorphous composite system and of μF and S2, over the full range of moisture content (m). **b** orthotropic swelling strains (ε_l) of μF and S2, in function of moisture content (m)

nounced in the longitudinal direction, where due to cellulose covalent bonds, the swelling coefficient is two orders of magnitude smaller ($\epsilon_z = 2 \times 10^{-3}$ at maximum moisture content) than in the other directions. This indicates that, for the microfibril systems, anisotropy directly results from the presence of crystalline cellulose that restrains most of the deformation in the direction of the crystal.

Porosity

The porosity of a structure is estimated by sampling the volume with a probe, after removing the adsorbed water, without changing the position of the atoms (Kulasinski et al. 2015a). Pore volume is defined as the void space between polymer chains which is large enough to accommodate spheres of given radius or molecules, here we use water molecule. Pore size distribution is probed by spheres of varying radius, i.e., starting with a radius of 1 nm and gradually decreasing the radius of the probe by an interval of 0.1 nm until reaching a radius of 0.1 nm (Fig. 9a). The total porosity is
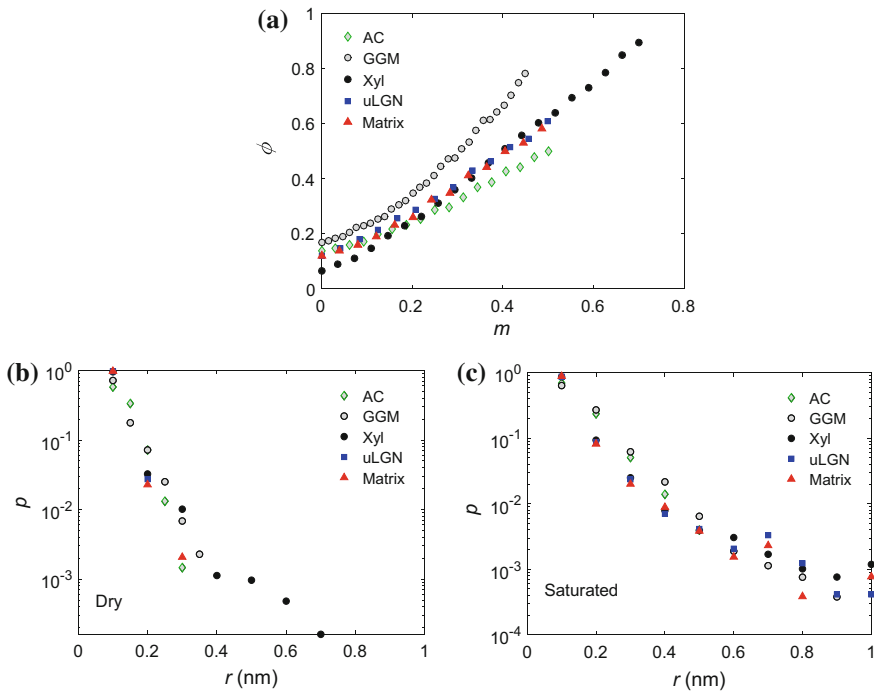

Fig. 9 **a** Porosity (ϕ) of homogeneous components and the amorphous composite as function of moisture content (m). Pores size distribution (p) of **b** dry and **c** saturated system, corresponding to moisture contents for AC 50%, GGM 44.8%, Xyl 70%, uLGN 48.5% and matrix 49%, in function of equivalent pore radius (r)

found to increase linearly with moisture content above 10% moisture content (MC). The rate of increase is higher for GGM and lower for AC, a trend which follows the swelling results presented above. The slower rate of increase seen below 10%MC is due to the initial porosity. The pores present initially are filled with water that is barely displacing the polymers as seen in Fig. 8. Once the initial porosity is occupied, any further water molecule absorption results in a displacement of the polymeric chains, thus yielding porosity and swelling strains to increase linearly. In contrast, in the first part of the curves, the swelling strains and porosity are increasing nonlinearly.

The pore size distribution for each system is given in dry and wet states (Fig. 9b, c). The profiles are very similar for all polymers in dry or in wet states. However, a general shift of the profile toward larger pore size is clearly observed.

Diffusion

MD allows for the careful observation of the displacement of water molecules within the polymeric systems at different moisture content. It is seen that water molecules alternate between hydrogen-bonded states with little displacement, or waiting time, and "free" movement with the systems. Waiting time is determined by measuring the length of the sections in mean square displacement when the deviation of the displacement from its average value is smaller than 0.1 nm (OH bond length) and the rate of change of its squared displacement is smaller than 8×10^{-8} nm^2 ns^{-1}. Bonding energy is calculated using transition state theory with waiting time and separately determined characteristic oscillation frequency (Kulasinski 2015d). Sorption sites, i.e., hydroxyls, are strongly polarized and this electrostatic attractiveness is conducive to the formation of hydrogen bonds, however, the presence of neighbor water molecules can mitigate this attractiveness. When a system holds few water molecules, a water molecule bonded to a sorption site on a polymeric chain is not perturbed by
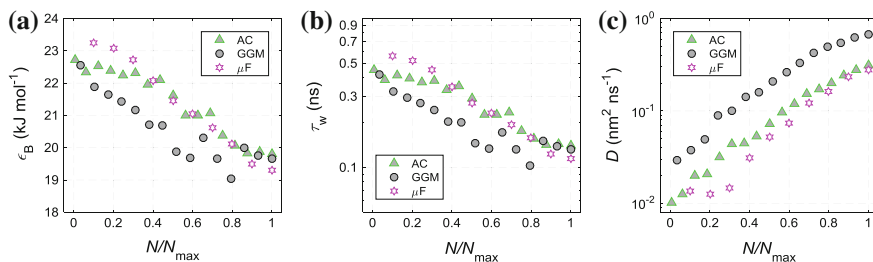

Fig. 10 **a** Bond energy of water with polymer, ε_B, **b** waiting time of bonded water molecule, τ_W, and **c** diffusion coefficient, D, versus normalized number of water molecules, where N_{max} is the maximum number of molecules that can be adsorbed in each system. N_{max} is determined from experimentally measured adsorption isotherms and is equal to 800, 2900, and 1000 for AC, HC, and μF, respectively (adapted from Kulasinski et al. 2015d)

neighbor water molecules, resulting in the hydrogen bond to be of higher bond energy and to undergo a longer waiting time, than seen of water–hydroxyl hydrogen bonds within water-abundant systems, as shown respectively in Fig. 10a, b. To calculate the diffusion coefficient, the mean square displacement (MSD) of the water molecules is followed over a sufficient time interval, i.e., larger than 1 ns, and its averaging, as per Einstein's equation, yields the diffusion coefficient. As the waiting time of bonded water molecules decreases, consequently, the global diffusion coefficient of water in the polymeric systems increases markedly with moisture content, Fig. 10c.

Mechanical Behavior

As moisture content increases, all investigated polymeric systems show a decrease in elastic moduli. In single systems, the decrease of the bulk moduli, determined by imposing tensile or compressive stress, is seen to be in the range of factor 3 or 4. Remarkably, the decrease in shear moduli is much more substantial, over one magnitude (Fig. 11a, b). These lower shear moduli at higher moisture content are in part due to the presence of water layers offering almost no resistance in shear. For anisotropic
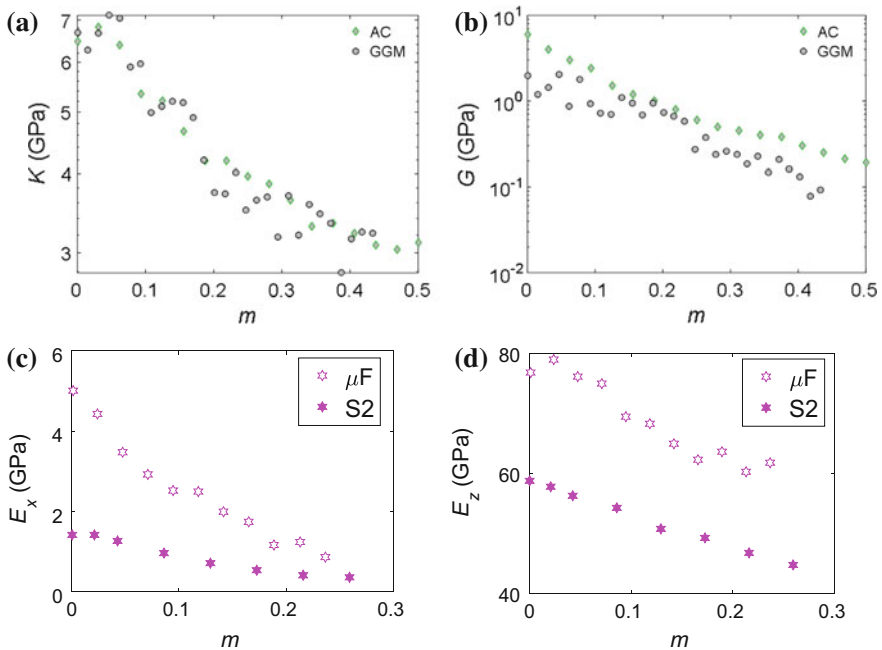

Fig. 11 Mechanical properties, **a** bulk (K) and **b** shear modulus (G) of AC and GGM, and Young's modulus of μF and S2 (E) **c** perpendicular and **d** parallel to crystalline cellulose, in function of moisture content (m) (adapted from Kulasinski 2015)

composite systems, Young's moduli are determined in the three principal directions. Results in the two directions x and y, perpendicular to the crystal orientation, are very similar. The weaker behavior with increasing moisture content is similar in all directions, but the magnitudes are very different for the behavior parallel to the crystal orientation (Fig. 11c, d). The difference between microfibril and S2 is in large part due to the lignin which makes about one-quarter of the S2 layer and which was here implemented with a low level of cross-polymerization, and as such is observed to weaken significantly.

Analysis Based on Hydrogen Bonds

Hydrogen bonds play a crucial role in the mechanical response of the polymeric systems studied here as they are exposed to increasing moisture content. As moisture content increases, hydrogen bonds linking polymer to polymer (HB[PP]) are broken to create space for the water molecules and the adsorption sites that thus become available can undergo hydrogen-bonding polymer to water (HB[PW]). As water content further increases, two water molecules in close neighborhood can also bond (HB[WW]). With higher water content, swelling occurs and porosity increases. Figure 12a shows the power-law relationship between normalized number of hydrogen bonds and porosity. Further, Fig. 12b presents the clear relationship between the normalized bulk and shear moduli and the number of polymer–polymer hydrogen bonds, indicating that hydrogen-bond breaking, due to water molecules adsorption, is directly responsible for the weakening of the mechanical behavior of the polymers, either amorphous cellulose or hemicellulose (GGM).
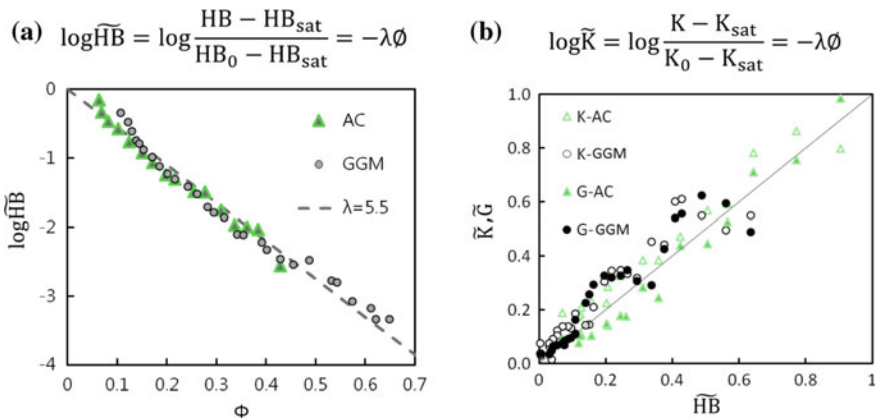

(a) $\log \widetilde{HB} = \log \dfrac{HB - HB_{sat}}{HB_0 - HB_{sat}} = -\lambda \emptyset$ **(b)** $\log \widetilde{K} = \log \dfrac{K - K_{sat}}{K_0 - K_{sat}} = -\lambda \emptyset$

Fig. 12 Relationships between normalized, denoted with tilde, **a** number of polymer–polymer hydrogen bonds (HB) and porosity (ϕ), where λ is the slope, and **b** bulk (K) and shear (G) moduli and number of hydrogen bonds (adapted from Kulasinski et al. 2015a)

Fig. 13 Isotherms of moisture content versus relative humidity (RH) for a deformable (black) and a rigid (red) AC samples, with circle for adsorption and triangle for desorption compared with experimental data blue (Mihranyan et al. 2004)
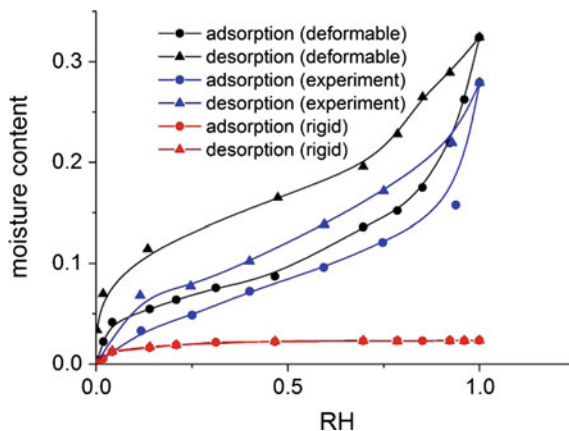
Hysteresis

Simulations of adsorption and desorption can be conducted in sequence following the GCMC approach described in section "Grand Canonical Monte Carlo". For the adsorption branch, dry AC is considered as initial configuration and several simulations are conducted at different chemical potentials to obtain the adsorption isotherm, shown with circles in Fig. 13. In desorption, the saturated state is the initial configuration and another series of simulations is conducted to obtain the desorption isotherm, as shown with triangle. Agreement with experiment (blue curves) is found acceptable. When the polymeric system is rigidly maintained in place, once the preexistent pores are filled, no further moisture sorption occurrs as shown in red. This result displays that absorption as seen in such polymers is possible due to the occurrence of material swelling. Also, moisture content versus volumetric strain is found to follow a linear relationship except at low moisture content range, where the curve is convex.

As AC is a non-crosslinked polymer, hydrogen bonds play a crucial role in both sorptive and deforming process and this is studied for both adsorption and desorption curves. When a water molecule is absorbed, it can form hydrogen bonds with either the sorption sites on the cellulose chains or with other present water molecules. Hydrogen bonds, formed between polymer to polymer (HB^{PP}), cellulose to water (HB^{PW}), and water to water (HB^{WW}), are counted at each moisture content states. Hysteresis in number of HB is found in all cases with more HB^{PP} and HB^{WW} in adsorption than desorption but with more HB^{PW} in desorption than adsorption. This can be attributed to the fact that more hydroxyl sites are exposed and become new adsorption sites because of the breakage of HB^{PP} as the moisture content increases.

Upscaling MD Results

MD simulations yield results that are analogous to experimentally determined behavior. Actually, there is a significant lack of information of the behavior of the constituents of wood and such information would be needed in multiscale modeling of the moisture behavior of wood from nanoscale to macroscale taking into consideration its constituents. To circumvent this scarcity, some multiscale works rely on micromechanics. Hofstetter et al. (2005) developed a continuum micromechanics multiscale model for softwood, where the elastic behavior of the cell wall material, composed of crystalline and amorphous cellulose embedded in polymer matrix, is estimated by a Mori-Tanaka scheme. Bader et al. (2011) extended this micromechanics framework to study the poroelastic role of water in the cell walls of softwoods. Following poro-micromechanics of multiphase materials, they estimated the effective poroelastic properties of softwood from a hierarchical set of matrix-inclusion problems at different length scales. Qing and Michnaevsky (2009) developed a multiscale finite element model to study the effects of microstructure on the moisture-related properties of softwood. Rafsanjani et al. (2013a) developed a multiscale model starting from the cell wall components and upscaled over cell wall to cellular structure and geometry, where they used for the lower scales the tri-layered structure of the cell wall. The material properties of the components came from previous experimental characterization and micromechanical homogenization. However, in all these approaches, strong assumptions and simplified modeling are made, in particular for the lower scale material behavior.

In a natural prolongation of the work, the MD material properties determined above can be parametrized and used directly to determine the properties of materials at higher scale using a poroelastic framework described below, removing the need to revolve to the many assumptions used in micromechanical modeling, in particular, the geometry of the inclusions and the absence of interface.

In a nanopore, the fluid is not in its bulk state as its molecules interact with the atoms of the polymer, thus being in an adsorbed state. For such nanoporous materials, conventional poromechanics breaks down. Brochard et al. (2012) developed an adequate poromechanical approach, where the equations are validated using GCMC simulations and applied the model to the case of methane adsorption in coal. There is still very little work along these lines where the actual interaction of the fluid in a nanoporous material, such as wood cell wall material, is taken into account. Nevertheless, the MD results of this chapter have successfully been upscaled to a poromechanical framework (Kulasinski et al. 2015a, b, c, d, Rafsanjani et al. 2015 following the methodology of Carmeliet et al. 2013). This model leads to the explicit formulation of the dependence of the poroelastic properties on mechanical loading and number of water molecules, as follows:

$$d\varepsilon = Cd\sigma + Bdn \tag{1}$$

$$d\mu = -Bd\sigma + M^{-1}dn, \tag{2}$$

Fig. 14 MD results (dots) and poroelastic model results (blue line) of undrained bulk modulus (K) in function of moisture concentration (n) (from Kulasinski et al. 2015b with permission)
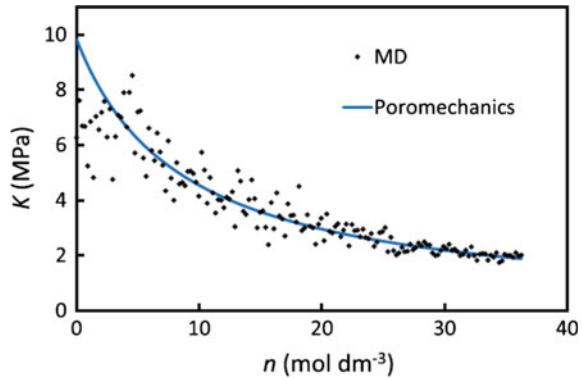
where ε is volumetric strain, C bulk compliance, σ volumetric stress, B a coupling coefficient, μ molar chemical potential, n molar concentration of water molecules, and M moisture capacity. To determine the necessary coefficients in the energy formulation, the MD results of adsorption, nonlinear swelling at zero stress and mechanical weakening of the bulk stiffness are used. The model can also describe mechano-sorptive effects, meaning sorption to be dependent on mechanical loading. Drained bulk modulus becomes stress dependent, even when the porous medium behaves linearly in undrained conditions. The poroelastic constitutive equations have been developed for a particular nanoporous material, amorphous cellulose, but this approach is generally applicable to the other components of wood or other materials (Fig. 14).

Outlook

The approach and work presented above allow detailed investigations of material behavior and physical phenomena. Only a small fraction of possibilities have been explored yet. Several paths are worthy and different scenarios could be tested. Possible outlook and perspectives could include:

1. Investigation of shape memory effect, another interesting hygromechanical behavior aside from swelling.
2. As computational capability grows, we can expect larger atomistic model, which reflects behaviors at larger scale, and reduces the disadvantages of present limited sized system.
3. Controlling chemical potential of water molecules, using the GCMC-MD hybrid method described above, for the determination of drained properties, which may also need longer simulations.
4. Keeping abreast of further chemical determination of the S2 polymeric constituents and configurations, including the shape of cellulose crystals (Fig. 15).
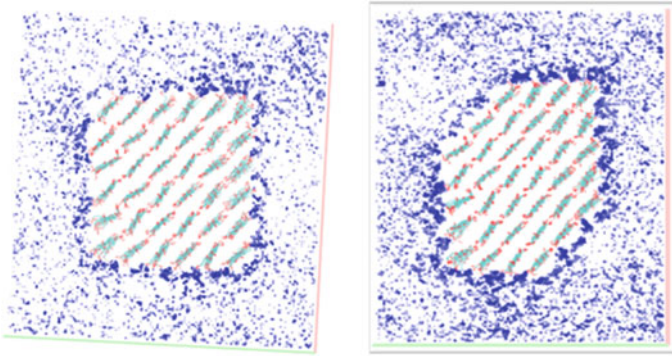
Fig. 15 Different water molecule profiles around two shapes of crystalline cellulose as example of further work. Crystalline cellulose is shown in cyan (carbon atom) and red (oxygen atom). Blue dots denote water molecule

5. Further development of a multiscale modeling framework from nano- to macroscale, with multiscale validation, combining experimental, MD and even mecoscopic modeling work.

Summary

Using atomistic modeling approach (molecular dynamics MD), we observed at nanoscale that, during adsorption of water molecules within hydrophilic polymers, water molecules first fill the existing pore space and afterwards displace the polymeric chains, leading to mostly linear swelling and weakening mechanical properties, in part due to the changes in hydrogen-bond network (Kulasinski et al. 2014b, 2015a, b, c, d). In addition to having demonstrated the capacity of MD to mimic macro phenomena at nanoscale, we show that 1. Moisture-related phenomena are scale-invariant, 2. HB dynamics play a key role in the control the moisture response, 3. Highly coupled phenomena are occurring. This work can lead to the construction of larger models, using MD as an input, to answer higher scale-related questions, such as shape memory effect known since long and seen experimentally at cellular scale in Derome et al. (2012).

Wood is almost ubiquitous as it is found in buildings structure, finishings, and furniture. Controlling swelling has been an everlasting challenge of the users of wood, therefore a better understanding of the swelling of wood can lead to better wood products design and longer durability. The understanding of the swelling of the S2 layer, a nanoporous composite material that interact strongly with moisture, can inspire the design of new materials where swelling would be desirable as with moisture-sensitive sensors, where anisotropy should be controlled either through careful design of the matrix, the fibrils or their interface, or where moisture-induced

shape memory would be aimed, taking benefit of a network of the fibrils. As source of raw material, cellulose crystals (nanowhiskers) and cellulose fibrils transformation are being industrialized and industrial-scale production is now thinkable. Thus, the investigation of S2 layer system could provide ideas and insights for the development of new functional nanomaterials, coatings, and nanocomposites, for a huge variety of engineering and other applications, including biomedical applications, using renewables. An ability to deform material during sorption of fluids offers a lot of possible applications related to enhanced environmental problems such as energy, climatic change, water, and CO_2 sequestration. Therefore, a fundamental understanding and modeling of sorption and its coupling to swelling and weakening are mandatory for their reliable implementation in engineering applications and the work presented in this chapter offer one promising way to achieve such understanding.

References

Bader T, Hofstetter K, Hellmich C, Eberhardsteiner J (2011) The poroelastic role of water in cell walls of the hierarchical composite softwood. Acta Mechanica 217:75–100

Beever DK, Valentine L (1958) Studies on the sorption of moisture by polymers. Part IV. Interval and integral sorption of water vapor by polymers. J Polym Sci A 32:521–522

Berendsen HJC, POstma JPM, van Gunsteren WF, DiNola ARHJ (1984) Molecular dynamics with coupling to an external bath. J Chem Phys 81(8):3684–3690

Boutelje JB (1962) The relationship of structure to transverse anisotropy in wood with reference to shrinkage and elasticity. Holzforschung 16:33–46

Brochard L, Vandamme M, Pellenq RJM (2012) Poromechanics of microporous media. J Mech Phys Solids 60:606–622

Carmeliet J, Derome D, Dressler M, Guyer R (2013) Nonlinear poro-elastic model for unsaturated porous solids. J Appl Mech 80(2):020909

Charlier L, Mazeau K (2012) Molecular modeling of the structural and dynamical properties of secondary plant cell walls: influence of lignin chemistry. J Phys Chem B 116(14):4163–4174

Cosgrove DJ (2014) Re-constructing our models of cellulose and primary cell wall assembly. Curr Opin Plant Biol 22:122–131

Derome D, Griffa M, Koebel M, Carmeliet J (2011) Hysteretic swelling of wood at cellular scale probed by phase-contrast X-ray tomography. J Struct Biol 173:180–190

Derome D, Rafsanjani A, Patera A, Guyer R, Carmeliet J (2012) Hygromorphic behaviour of cellular material: hysteretic swelling and shrinkage of wood probed by phase contrast X-ray tomography. Phil Mag 92:3680–3698

Dinwoodie JM (2000) Timber, its nature and behaviour, 2nd. E & FN Spon, London, New York, England

Eichhorn S (2011) Cellulose nanowhiskers: promising materials for advanced applications. Soft Matter 7:303–315

Fahlén J, Salmén L (2005) Pore and matric distribution in the fiber wall revealed by atomic force microscopy and image analysis. Biomacromol 6(1):433–438

Forest Products Laboratory (2010) Wood handbook—wood as an engineering material. General Technical Report FPL-GTR-190. Madison, WI: U.S. Department of Agriculture, Forest Service, Forest Products Laboratory, 508 p

Hess B, Kutzner C, Van Der Spoel D, Lindahl E (2008) GROMACS 4: algorithms for highly efficient, load balanced, and scalable molecular simulation. J Chem Theory Comput 4:435–447

Hofstetter K, Hellmich C, Eberhardsteiner J (2005) Development and experimental validation of a continuum micromechanics model for the elasticity of wood. Eur J Mech A/Solids 24:1030–1053

Höfter H, Gonneau M, Vernhettes S (2007) 2.22 Biosynthesis of cellulose. In: Kalerming H (ed) Comprehensive glycoscience. Oxford Elsevier, pp 737–763

Jin K, Qin Z, Buhler M (2015) Molecular deformation mechanisms of the wood cell wall material. J Mech Behav Biomed Mater 42:198–206

Kulasinski K (2015) Physical and mechanical aspects of moisture adsorption in wood biopolymers investigated with atomistic simulations. Dissertation ETH No. 23046, ETH Zurich

Kulasinski K, Keten S, Churakov SV, Derome D, Carmeliet J (2014a) A comparative molecular dynamics study of crystalline, paracrystalline and amorphous states of cellulose. Cellulose 21:1103–1116

Kulasinski K, Keten S, Churakov S, Guyer R, Derome D, Carmeliet J (2014b) Molecular mechanism of moisture-induced transition in amorphous cellulose. ACS Macro Lett 3:1037–1040

Kulasinski K, Guyer R, Keten S, Derome D, Carmeliet J (2015a) Impact of moisture adsorption on structure and physical properties of amorphous biopolymers. Macromolecules 48:2793–2800

Kulasinski K, Guyer R, Derome D, Carmeliet J (2015b) Poroelastic model for adsorption-induced deformation of biopolymers obtained from molecular simulations. Phys Rev E 92:022605

Kulasinski K, Guyer R, Derome D, Carmeliet J (2015c) Water adsorption in wood microfibril: role of the crystalline-amorphous cellulose. Biomacromol 16:2972–2978

Kulasinski K, Guyer R, Derome D, Carmeliet J (2015d) Water diffusion in hydrophilic systems: a stop and go process. Langmuir 31:10843–10849

Lins RD, Hünenberger PH (2005) A new GROMOS force field for hexopyranose-based carbohydrates. J Comput Chem 26:1400–1412

Mihranyan A, Llogostera AP, Karmhag R, Stromme M, Ek R (2004) Moisture sorption by cellulose powders of varying crystallinity. Int J Pharm 269(2):433–442

Neuhaus FH (1981) Elastizitätszahlen von Fichtenholz in Abhängigkeit von der Holzfeuchtigkeit. PhD thesis, Ruhr-Universität Bochum, Bochum, Germany

Nishiyama Y, Langan P, Chanzy H (2002) Crystal structure and hydrogen-bonding system in cellulose Iβ from synchrotron X-ray and neutron fiber diffraction. J Am Chem Soc 124:9074–9082

Oostenbrink C, Villa A, Mark AE, Van Gunsteren WF (2004) A biomolecular force field based on the free enthalpy of hydration and solvation: the GROMOS force-field parameter sets 53A5 and 53A6. J Comput Chem 25:1656–1676

Patera A (2014) 3D experimental investigation of the hygro-mechanical behaviour of wood at cellular and sub-cellular scales. Diss. ETH no. 22230, ETHZ, Zurich

Patera A, Derome D, Griffa M, Carmeliet J (2013) Hysteresis in swelling and in sorption of wood tissue. J Struct Biol 182:226–234

Petridis L, Schulz R, Smith JC (2011a) Simulation analysis of the temperature dependence of lignin structure and dynamics. J Am Chem Soc 133:20277–20287

Petridis L, Pingali SV, Urban V, Heller WT, O'Neill HM, Foston M, Smith JC (2011b) Self-similar multiscale structure of lignin revealed by neutron scattering and molecular dynamics simulation. Phys Rev E 83(6):061911

Petridis L, Smith JC (2009) A molecular mechanics force field for lignin. Comp Chem 30:457–467

Plimpton S (1995) Fast parallel algorithms for ahort-range molecular dynamics. J Comput Phys 117:1–19

Qing H, Mishnaevsky L (2009) Moisture-related mechanical properties of softwood: 3D micromechanical modeling. Comput Mater Sci 46:310–320

Rafsanjani A, Derome D, Carmeliet J (2013a) Micromechanics investigation of hygro-elastic behavior of cellular materials with multi-layered cell walls. Compos Struct 95:607–611

Rafsanjani A, Lanvermann Derome D, Niemz P, Carmeliet J (2013b) Multiscale analysis of free swelling of Norway spruce. Compos Part A Appl Sci Manuf 54:70–78

Rafsanjani A, Stiefel M, Jefimovs K, Mokso R, Derome D, Carmeliet J (2014) Hygroscopic swelling of latewood cell wall micropillars reveals ultra-structural anisotropy. Interface 11:20140126

Rafsanjani A, Derome D, Carmeliet J (2015) Poromechanical modeling of moisture induced swelling anisotropy of cellular tissues of softwoods. RCS Adv 5:3560–3566

Salmén L (2004) Micromechanical understanding of the cell-wall structure. C.R. Biologies 327:873–880

Salmén L, Burgert I (2009) Cell wall features with regard to mechanical performance. A review. Cost action E35 2004-2008: wood machining—micromechanics and fracture. Holzforschung 63:121–129

Sangha AK, Petridis L, Smith JC, Ziebell A, Parks JM (2012) Molecular simulation as a tool for studying lignin. Environ Prog Sustain Energy 31(1):47–54

Smith PE, van Gunsteren WF (1994) Consistent dielectric properties of the simple point charge and extended simple point charge water models at 277 and 300 K. J Chem Phys 100:3169–3174

Sun H, Mumby SJ, Maple JR, Hagler AT (1994) An ab Initio CFF93 all-atom force field for polycarbonates. J Am Chem Soc 116:2978–2987

Teleman O, Jönsson B, Engström S (1987) A molecular dynamics simulation of a water model with intramolecular degrees of freedom. Mol Phys 60:193–203

Wagenführ A, Scholz F (2012) Taschenbuch des Holztechnik. Carl Hanser Verlag, Munich

Watanabe U, Norimoto M, Morooka T (2000) Cell wall thickness and tangential Young's modulus in coniferous early wood. J Wood Sci 46:109–114

Xu P, Donaldson LA, Gergely ZR, Staehelin LA (2007) Dual-axis electron tomography: a new approach for investigating the spatial organization of wood cellulose microfibrils. Wood Sci Technol 41:101–116

Zwanzig RW (1954) High-temperature equation of state by a perturbation method. I. nonpolar gases. J Chem Phys 22:1420–1426